PERGAMON

Available online at www.sciencedirect.com

SCIENCE DIRECT®

Computers and Structures 80 (2002) 2483–2493

Computers & Structures

www.elsevier.com/locate/compstruc

Push-over analysis for performance-based seismic design

R. Hasan, L. Xu, D.E. Grierson *

Department of Civil Engineering, University of Waterloo, Waterloo, Ont., Canada N2L 3G1

Received 6 August 2001; accepted 22 July 2002

Abstract

The paper presents a simple computer-based push-over analysis technique for performance-based design of building frameworks subject to earthquake loading. The technique is based on the conventional displacement method of elastic analysis. Through the use of a 'plasticity-factor' that measures the degree of plastification, the standard elastic and geometric stiffness matrices for frame elements (beams, columns, etc.) are progressively modified to account for nonlinear elastic–plastic behavior under constant gravity loads and incrementally increasing lateral loads. The behavior model accounts for material inelasticity due to both single and combined stress states, and provides the ability to monitor the progressive plastification of frame elements and structural systems under increasing intensity of earthquake ground motion. The proposed analysis technique is illustrated for two building framework examples.

Keywords: Push-over analysis; Steel frames; Seismic loading

1. Introduction

While conventional limit-states design is typically a two-level design approach having concern for the service-operational and ultimate-strength limit states for a building, performance-based design can be viewed as a multi-level design approach that additionally has explicit concern for the performance of a building at intermediate limit states related to such issues as occupancy and life-safety standards. With the emergence of the performance-based approach to design, there is a need to develop corresponding analysis tools. Nonlinear static (push-over) analysis is often an attractive choice in this regard because of its simplicity and ability to identify component and system-level deformation demands with accuracy comparable to dynamic analysis [5,11,12,14,17].

The present study develops a push-over analysis procedure based on a continuous nonlinear post-elastic material model, which provides the capacity to monitor initial yielding and gradual progressive plastic behavior of both individual elements and overall structural systems. The procedure is applicable for the inelastic analysis of building frameworks having ideal 'rigid' or 'pinned' connections, and is adapted from a procedure originally conceived for the elastic analysis of frame structures having 'semi-rigid' connections. A potential 'plastic-hinge section' of a frame member is treated as a 'pseudo-semi-rigid connection' with predefined nonlinear load-deformation characteristics. The computational push-over analysis procedure is a formal algorithm for nonlinear inelastic analysis of rigid frameworks that proceeds exactly as for nonlinear elastic analysis of semi-rigid frameworks. The principles of semi-rigid analysis and their extension to post-elastic analysis are first presented in the following. The proposed push-over analysis procedure is then presented, and corresponding computational details are illustrated for two example building frameworks.

2. Semi-rigid analysis

In an early study concerning semi-rigid frame analysis, [15] modeled the moment-connection at each end $i = 1, 2$ of a planar beam-column member as a linear spring, Fig. 1, and introduced the nondimensional 'rigidity-factor',

* Corresponding author.

0045-7949/02/$ - see front matter
PII: S0045-7949(02)00212-2

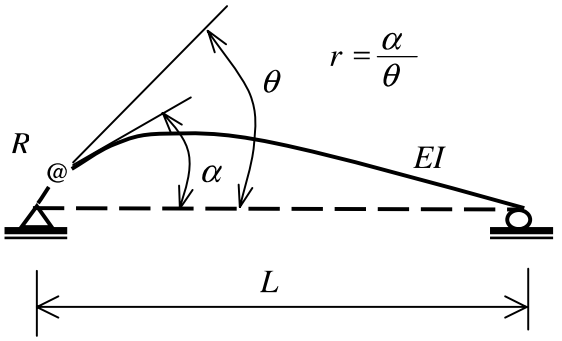

Fig. 1. Semi-rigid moment-connection.

$$r_i = \frac{\alpha_i}{\theta_i} = \frac{1}{1 + (3EI/R_iL)} \quad (i = 1, 2) \tag{1}$$

where R_i is the rotational stiffness of connection i, and EI and L are the bending stiffness and length of the connected member, respectively. The rigidity-factor r_i defines the rotational stiffness of the connection relative to that of the attached member and, as shown in Fig. 1, can be interpreted as the ratio of the end-rotation α_i of the member to the combined rotation θ_i of the member and the connection. From Eq. (1), the rigidity-factor falls in the range between $r_i = 1$ and $r_i = 0$ as the connection stiffness varies between $R_i = \infty$ and $R_i = 0$, respectively (infinite stiffness implies that the connection is perfectly 'rigid' in the sense that it fully preserves continuity of elastic deformation, while zero stiffness implies that the connection is perfectly 'pinned' in the sense that it freely allows discontinuity of elastic deformation).

Monfortoon and Wu employed the rigidity-factor concept to develop a first-order elastic analysis technique for semi-rigid frames, where the elastic stiffness matrix $\boldsymbol{K}$ of each member with 'semi-rigid' moment-connections is found as the product of the standard elastic stiffness matrix $\boldsymbol{S}_e$ for a member having 'rigid' moment-connections and a correction matrix $\boldsymbol{C}_e$ formulated as a function of the rigidity-factors r for the two end-connections, i.e.,

$$\boldsymbol{K} = \boldsymbol{S}_e \boldsymbol{C}_e \tag{2}$$

Xu [20] further employed the rigidity-factor concept to develop a second-order elastic analysis technique for semi-rigid frames. Here, for each member with 'semi-rigid' moment-connections, the standard geometric stiffness matrix $\boldsymbol{S}_g$ for a member with 'rigid' moment-connections is modified by a correction matrix $\boldsymbol{C}_g$ formulated as a function of the rigidity-factors r for the two end-connections. The member elastic stiffness matrix $\boldsymbol{K}$ accounting for both first-order elastic and second-order geometric properties is then found as, from Eq. (2),

$$\boldsymbol{K} = \boldsymbol{S}_e \boldsymbol{C}_e + \boldsymbol{S}_g \boldsymbol{C}_g \tag{3}$$

The matrices $\boldsymbol{C}_e$ and $\boldsymbol{C}_g$ appearing in Eqs. (2) and (3) are illustrated in Appendix A for a planar beam-column member having semi-rigid moment-connections.

Having the nonlinear moment-rotation relations that characterize the variation in rotational stiffness R of semi-rigid connections under increasing moment (see [21]), the influence of semi-rigid connection behavior on the overall behavior of a frame structure under increasing loads can be directly accounted for through an incremental load analysis. Here, for each finite load increment, the stiffness R of each connection is held constant at its value prevailing at the beginning of the load step and the conventional displacement method of elastic analysis is applied for rigidity-factors r found through Eq. (1) and member stiffness matrices $\boldsymbol{K}$ found through Eq. (2) or Eq. (3), to find the corresponding increments of moments and rotations for the structure.

3. Post-elastic analysis

Push-over analysis monitors the progressive stiffness degradation of a frame structure as it is loaded into the post-elastic range of behavior. Based on the rigidity-factor concept described in the foregoing for semi-rigid analysis, this study proposes to use a 'plasticity-factor' to monitor the progressive plastification (stiffness degradation) of frame members under increasing loads. Specifically, any potential 'plastic-hinge section' is treated as a 'pseudo semi-rigid connection' whose stiffness variation is measured by a plasticity-factor p that ranges from unity (ideal elastic) to zero (fully plastic). As described in the following, a generic moment–curvature relation is adopted to characterize the nonlinear variation in post-elastic flexural stiffness of plastic-hinge sections under increasing moment.

The post-elastic degradation of the flexural stiffness of a frame member begins when the material fibers furthest from the neutral axis of the cross-section experience initial yielding and, under increasing moment, continues as plasticity spreads through the section depth and along the member length to form a fully-developed plastic hinge, at which point the flexural stiffness of the member section is exhausted. This degradation in section stiffness beyond the linear-elastic range of behavior is characterized by a nonlinear moment–curvature (M–ϕ) curve of the form shown in Fig. 2, where Φ_y is the known curvature when the extreme fibers of the member section experience initial yielding, ϕ_p is the known post-elastic curvature increment beyond Φ_y when plasticity first penetrates through the full depth of the cross-section, and ϕ_u is the known post-elastic curvature increment beyond Φ_y when the section reaches an ultimate deformation state corresponding to abrupt loss of some or all of its flexural strength (e.g., buckling of the compression flange of a wide-flange steel beam section). With little error for most section shapes used in building frame-

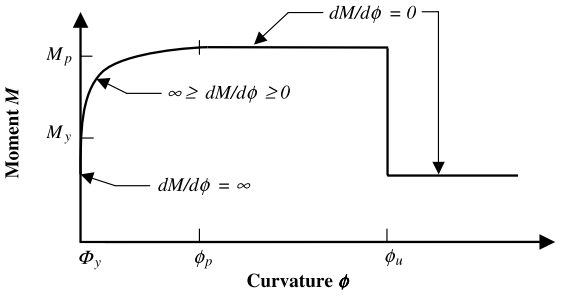

Fig. 2. Post-elastic moment–curvature relation.

works, it can be assumed that the continuous nonlinear portion of this generic M–ϕ curve has an elliptical shape that is defined by the function,

$$M(\phi) = M_y + \sqrt{(M_p - M_y)^2 - ((M_p - M_y)(\phi - \phi_p)/\phi_p)^2} \tag{4}$$

In Eq. (4), $M_y = S\sigma_y$ and $M_p = Z\sigma_y$ are the known first-yield and fully-plastic moment capacities of the member section, respectively (S and Z are the elastic and plastic section moduli, respectively, and σ_y is the expected yield stress of the material), and ϕ is the post-elastic curvature increment beyond Φ_y at any stage between initial yielding ($\phi = 0$) and full plastification ($\phi = \phi_p$) of the cross-section. From Eq. (4), the post-elastic moment varies in the range $M_y \leqslant M(\phi) \leqslant M_p$ as the post-elastic curvature increment varies in the range $0 \leqslant \phi \leqslant \phi_p$.

From Fig. 2, for moment levels less than M_y the change in post-elastic curvature $d\phi = 0$ and the post-elastic section flexural stiffness $dM/d\phi = \infty$ (infinite stiffness implies that the member section fully preserves continuity of elastic deformation). Conversely, beyond the point on the M–ϕ curve where the moment level reaches M_p the change in post-elastic moment $dM = 0$ and the post-elastic section flexural stiffness $dM/d\phi = 0$ (zero stiffness implies that the member section has fully formed a plastic hinge that freely allows rotational discontinuity). That is, the post-elastic flexural stiffness varies in the range $\infty \geqslant dM/d\phi \geqslant 0$ as the cross-section behavior progresses from initial yielding at the M_y moment level ($\phi = 0$) to full plastification at the M_p moment level ($\phi = \phi_p$) and, upon differentiating Eq. (4) with respect to ϕ, is defined by the function,

$$\frac{dM(\phi)}{d\phi} = \frac{(M_p - M_y)^2(\phi_p - \phi)}{\phi_p^2\sqrt{(M_p - M_y)^2 - ((M_p - M_y)(\phi - \phi_p)/\phi_p)^2}} \tag{5}$$

From the foregoing, there is evident mathematical similarity between the model for post-elastic behavior of a plastic-hinge section and that for the elastic behavior of a semi-rigid connection. In fact, upon replacing connection rotational stiffness R with section flexural stiffness $dM/d\phi$ in Eq. (1), the degradation of the flexural stiffness of a member section experiencing post-elastic behavior can be characterized by the 'plasticity-factor',

$$p = \frac{1}{1 + (3EI/(dM/d\phi)L)} \tag{6}$$

which varies in the range $1 \geqslant p \geqslant 0$ as the post-elastic flexural stiffness varies between that for an ideal elastic ($dM/d\phi = \infty$) and fully plastic ($dM/d\phi = 0$) section, respectively. Further, upon replacing rigidity-factor r with plasticity-factor p in the matrices $\boldsymbol{C}_s$ and $\boldsymbol{C}_g$ of Eqs. (2) and (3) that define member stiffness matrix $\boldsymbol{K}$ (e.g., see Appendix A), the influence of post-elastic section behavior on the overall behavior of a frame structure under increasing loads can be directly accounted for through an incremental-load analysis procedure similar to that for elastic semi-rigid analysis, as described in the following:

1. Member stiffness matrices are defined by Eq. (3) or Eq. (2), depending on whether or not second-order behavior is to be accounted for.
2. The finite load increment is taken arbitrarily small so that all member sections of the structure exhibit elastic behavior ($p = 1$, $\phi = 0$) during the initial stage of the loading history. (The small increment also ensures that all plastic behavior is accurately identified over the loading history, including at the end when plastic collapse of the structure occurs—see point 10.)
3. The post-elastic flexural stiffness $dM/d\phi$ of each member section is held constant at its value prevailing at the beginning of each load step. (As well, the post-elastic response is maintained monotonic over the load step in the sense that any occurrence of elastic unloading does not result in stiffness recovery at any member section previously exhibiting plastic behavior—this ensures that plasticity-related damage is not artificially reduced or eliminated during the analysis process.)
4. Upon incrementing the loads, the displacement method of analysis is applied to find the (accumulated) value of each section moment M at the next load level.
5. If $M \leqslant M_y$ then $\phi = 0$; otherwise, if $M > M_y$ then Eq. (4) is solved for $M(\phi) = M$ to find the corresponding value of the post-elastic curvature for the section as,

$$\phi = \phi_p - \phi_p\sqrt{1 - \left(\frac{M - M_y}{M_p - M_y}\right)^2} \tag{7}$$

6. In turn, the ϕ value from Eq. (7) is substituted into Eq. (5) to update the post-elastic flexural stiffness $dM/d\phi$ of the member section to its value prevailing at the beginning of the next load step (note that if $\phi \geqslant \phi_u$ from Eq. (7) then $\phi = \phi_p$ is substituted into Eq. (5) so that, as shown in Fig. 2, $dM/d\phi = 0$ remains the case even after the moment level abruptly

decreases due to a partial or complete local failure of the section).

7. The updated $dM/d\phi$ value is used to update the section plasticity-factor p through Eq. (6). At any stage of the analysis process, the factor p may be used to estimate the corresponding percentage extent of section plastic behavior through the expression,

$$\% \text{ Plasticity} = 100(1-p) \tag{8}$$

8. The updated plasticity factor values p_i $(i = 1, 2)$ at the two end-sections of each member are used to update the member stiffness matrix $\boldsymbol{K}$ through Eq. (2) or Eq. (3).
9. The structure stiffness matrix is updated and the analysis procedure is repeated for the next load increment.
10. The plastification of member sections ($p < 1$) is progressively traced over the incremental-load history until the load level is reached at which a sufficient number of fully-developed plastic hinges ($p = 0$) have formed as to exhaust the stiffness of the structure, in whole or in part (i.e., the structure stiffness matrix becomes singular, which signifies formation of a plastic-collapse failure mechanism).

Though the foregoing refers to the pure bending case, the post-elastic analysis procedure is readily extended to account for combined stress states. For example, consider the case of combined bending moment M and axial force N for members of planar frameworks. The reduction in the moment capacity of a member cross-section due to the presence of axial force can be accounted for through the following interaction constraint equation, having lower and upper bounds that correspond to first-yield and fully-plastic behavior, respectively,

$$\frac{1}{f} \leqslant \frac{M}{M_{\mathrm{p}}} + \left[\frac{N}{N_{\mathrm{p}}}\right]^{m} \leqslant 1.0 \tag{9}$$

where, for the member section, $f = M_{\mathrm{p}}/M_y = Z/S$ is the shape factor (e.g., $f = 1.12$–1.16 for wide-flange steel beam sections), $N_{\mathrm{p}} = A\sigma_y$ is the fully-plastic axial force capacity (where A is the cross-section area) and the exponent m depends on the section shape (e.g., $m = 2$ for a rectangular section). The lower bound for Eq. (9) defines the first-yield axial force capacity of a member section to be $N_y = (1/f)^{1/m} N_{\mathrm{p}}$.

Taking $m = 1$ for the sake of illustration, the two bounds for Eq. (9) can be viewed as defining the shaded 'plasticity domain' shown in Fig. 3. Assuming that the ratio M/N remains constant in the post-elastic response range, identical satisfaction of the lower bound of Eq. (9) at generic point O_y in Fig. 3 corresponds to first-yield behavior occurring at the reduced yield moment level $M_y^r = M_{\mathrm{p}}/nf$ (where $n > 1$), while identical satisfaction of the upper bound of Eq. (9) at related point O_{p} in Fig. 3 corresponds to fully-plastic behavior occurring at the reduced plastic moment level $M_{\mathrm{p}}^r = M_{\mathrm{p}}/n = fM_y^r$. Upon replacing M_y and M_{p} with the reduced moments M_y^r and M_{p}^r, Eqs. (4) and (5) then respectively define post-elastic moment–curvature and flexural-stiffness relations that account for the influence of axial force on bending moment capacity of member sections, and the post-elastic analysis procedure can proceed exactly as described in the foregoing for the pure bending case.

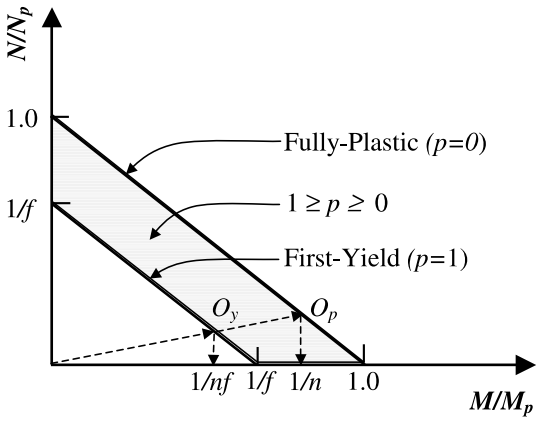

Fig. 3. Plasticity under combined bending moment and axial force.

4. Proposed push-over analysis

Conventional push-over analysis performed in the context of performance-based seismic design is a computational procedure where, for static-equivalent loading consisting of constant gravity loads and monotonically increasing lateral loads, the progressive stiffness/strength degradation of a building framework is monitored at specified performance levels. The analysis procedure is approximate in that it represents a multi-degree-of-freedom (MDOF) building system by an equivalent single-degree-of-freedom (SDOF) system [2,17]. The fundamental mode of vibration of the MDOF system is often selected as the response mode of the equivalent SDOF system. The selected vibration response mode is the basis for estimating the distribution of static-equivalent lateral inertia loads applied over the height of the building.

Specified deformation states are often taken as a measure of building performance at corresponding load levels [19]. For example, the US Federal Emergency Management Agency [6] identifies operational, immediate-occupancy, life-safety and collapse-prevention performance levels, and adopts roof-level lateral drift at

the corresponding load levels as a measure of the associated behavior states of the building. The increasing degrees of damage that a building experiences at the various performance levels are associated with earthquakes having increasing intensities of horizontal ground motion (see examples).

The horizontal ground motion intensity of an earthquake defines the spectral response acceleration S_a of a building in the lateral direction, which may be transformed into a total horizontal base shear force as [4],

$$V = \frac{S_a}{g} W \tag{10}$$

where g is the gravitational constant and W is the total weight of the building. The shear force V is in equilibrium with a distribution of lateral inertia forces F applied over the vertical height of the building, which, for example, FEMA [6] defines as,

$$F_x = C_{vx} V \tag{11a}$$

$$C_{vx} = \frac{w_x h_x^k}{\sum_{i=1}^{n} w_i h_i^k} \tag{11b}$$

where F_x is the lateral load applied at story level x, and C_{vx} is the corresponding vertical distribution factor defined by: gravity loads w_x and w_i = the portions of the total building weight at story levels x and i, respectively; vertical distances h_x and h_i = the heights from the base of the building to story levels x and i, respectively; the total number n of stories; and an exponent k whose value depends on the fundamental period of the building.

The push-over analysis proposed by this study is based on the post-elastic analysis procedure described in Section 3. The procedural steps are here illustrated for the four building performance levels [6] mentioned in the foregoing and indicated in the flow chart shown in Fig. 4. The structure data describes the dimensions and numbers of bays and stories (L, h, n, etc.) and the types of connections and supports (fixed, pinned, etc.) for the building. The member data describes the cross-section properties for the beams, columns and other structural components of the building (A, E, I, S, Z, m, σ_y, Φ_y, ϕ_p, ϕ_u, etc.). The load data describes the gravity loads and building weight (w, W), as well as the distribution of incremental lateral inertia loads ΔF precalculated through Eqs. (10)–(11b) for arbitrarily small spectral acceleration S_a and prescribed exponent k (see Examples). The performance data describes the parameters that quantify the performance levels for the building. For this study, the operational performance level is associated with the onset of initial yielding; i.e., all $p = 1$ and $M = M_y$ or M_y^r for at least one member section of the building. The immediate-occupancy, life-safety and collapse-prevention performance levels are associated

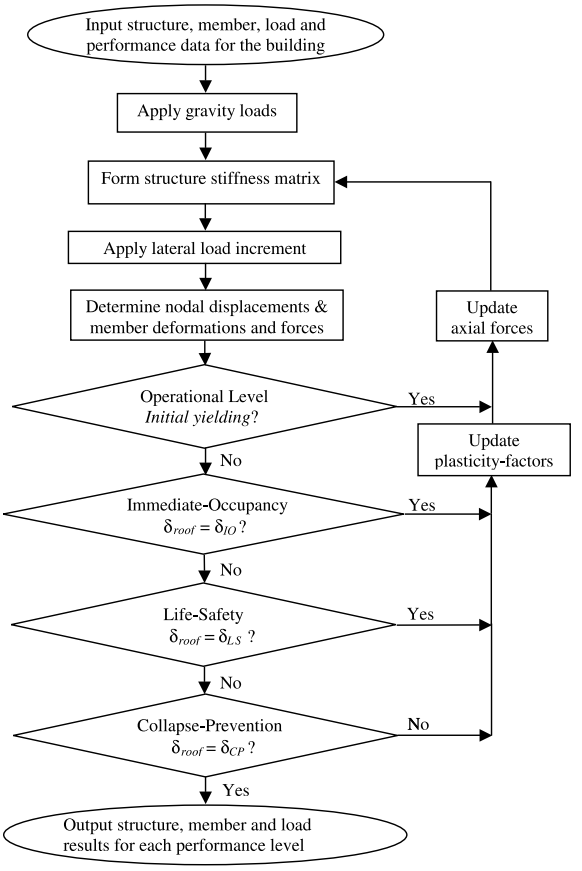

Fig. 4. Push-over analysis flow chart.

with the building reaching corresponding target roof-level lateral displacements δ_{IO}, δ_{LS} and δ_{CP}, respectively (see Examples).

The gravity loads on the building remain constant for the analysis. The structure stiffness matrix is initially formed by member stiffness matrices defined by Eq. (2) assuming linear elastic behavior of the building (all $p = 1$). After each lateral load increment the structure stiffness matrix is formed by member stiffness matrices defined by Eq. (3), for updated plasticity factors ($p < 1$) from Eq. (6) and updated axial forces ($N \neq 0$) from the analysis results, to account for nonlinear post-elastic behavior and second-order geometric stiffness effects (see Appendix A), under single or combined stresses (e.g., see Eq. (9)). The lateral loads are progressively increased through the different performance levels until the lateral displacement at the roof level of the building reaches the target value associated with the collapse-prevention level ($\delta_{roof} = \delta_{CP}$), at which point the push-over analysis terminates. The structure, member and load results found at each building performance level are provided as output from the analysis. The lateral nodal displacements reached at each performance level define the

corresponding overall and interstory ductility demands (DD) imposed on the building, i.e.

$$\text{Overall DD}_{\text{roof}} = \frac{\delta_{\text{roof}}}{\delta_{\text{yield}}} \tag{12a}$$

$$\text{Interstory DD}_x = \frac{\delta_x - \delta_{x-1}}{(\delta_x - \delta_{x-1})_{\text{yield}}} \tag{12b}$$

where δ_{yield} = roof lateral displacement at the operational performance level defined by the onset of initial yielding of the structure, δ_{roof} = roof lateral displacement δ_{yield}, δ_{IO}, δ_{LS} or δ_{CP} depending on the performance level of concern, $\delta_x - \delta_{x-1}$ = interstory drift of story x at the performance level of concern (δ_x and δ_{x-1} = lateral displacements at story-levels x and $x-1$, respectively), and $(\delta_x - \delta_{x-1})_{\text{yield}}$ = interstory drift of story x at the loading level when initial yielding of the story occurs (i.e., $p = 1$ for all members comprising the story, but $M = M_y$ or M_y^r for at least one member section). The push-over analysis results at each building performance level also include the corresponding spectral acceleration $S_a^{\text{analysis}} = Vg/W$ calculated through Eq. (10), where the base shear force V is equal to the total of the lateral loads applied at the performance level.

5. Examples

Consider the three-story and nine-story steel moment-frames shown in Figs. 5 and 6. These frames have been previously studied in the literature and, unless noted or referenced otherwise, the data and information ascribed to them in the following is due to [9,10]. The two frameworks have rigid moment-connections and fixed supports, and are perimeter frames of buildings designed in accordance with the earthquake provisions of the Uniform Building Code [18]. The fundamental period for the three-story frame is 1.01 s, while that for the nine-story frame is 2.34 s.

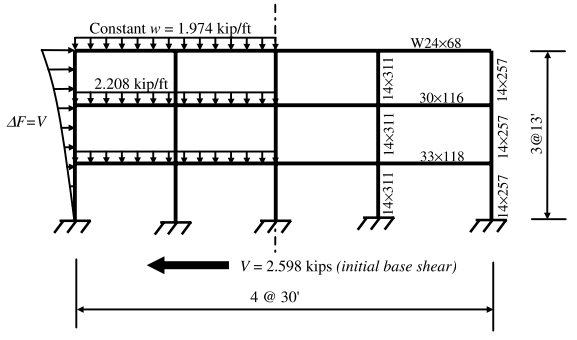

Fig. 5. Three-story steel moment-frame.

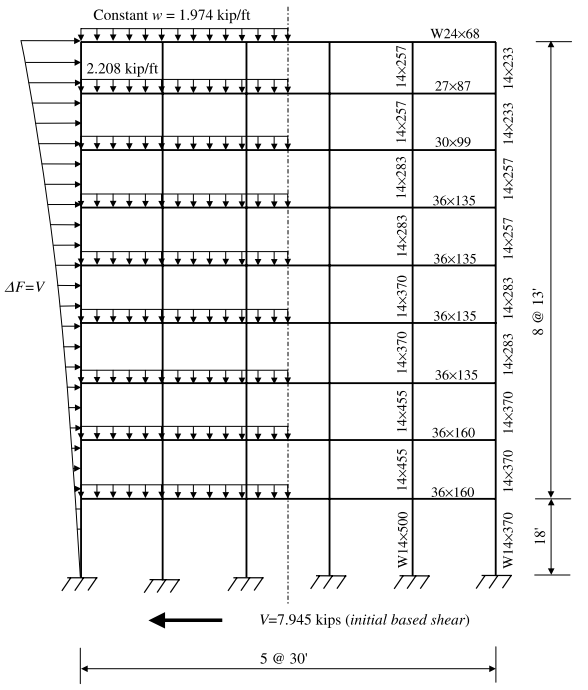

Fig. 6. Nine-story steel moment-frame.

The properties of each of the different W-shape beam and column members indicated in Figs. 5 and 6 are available in manuals of the American Institute of Steel Construction [1], and include the elastic modulus E and expected yield stress σ_y of the material and the area A, moment of inertia I, elastic modulus S and plastic modulus Z of the cross-section. The post-elastic curvature increment beyond the first-yield curvature Φ_y when plasticity first penetrates through the full depth of a member cross-section is taken to be $\phi_{\text{p}} = 0.045$ radians [3], while the value of the ultimate post-elastic curvature increment ϕ_{u} is set arbitrarily large so that member sections do not experience abrupt local failure (see Fig. 2). The combined influence of bending moment M and axial force N on plastic behavior is accounted for through Eq. (9) for exponent $m = 1$ (see Fig. 3).

The constant gravity load intensities w indicated for the roof and floor beams in Figs. 5 and 6 include account for a tributary-area width of 15 feet and dead-load and live-load factors of 1.2 and 1.6, respectively [1]. As indicated in Table 1, the initial base shear forces V shown in Figs. 5 and 6 are calculated through Eq. (10) for an arbitrarily small spectral acceleration $S_a = 0.0008g$ and given story weights w_x (which, at each story level x, include account for a tributary area equal to one-half the floor plan of the building, while w_x at the roof level also accounts for a penthouse). The individual story-level lateral load increments ΔF_x indicated in Table 1 are calculated through Eqs. (11a) and (11b) for ex-

Table 1
Story-level distribution of lateral load increments

Building	Story level (x)	Story weight w_x (kip)	Initial base shear $V = 0.0008\ \Sigma w_x$ (kip)	Distribution factors C_{vx} [Eq. (11b)]	Load increments $\Delta F_x = C_{vx} V$ (kip)
Three-story	1	1054	2.598	0.068	0.177
	2	1054		0.271	0.704
	Roof	1140		0.661	1.717
Nine-story	1	1111	7.945	0.006	0.048
	2	1092		0.017	0.135
	3	1092		0.035	0.278
	4	1092		0.059	0.469
	5	1092		0.089	0.707
	6	1092		0.124	0.985
	7	1092		0.166	1.319
	8	1092		0.215	1.708
	Roof	1176		0.289	2.296

Table 2
Push-over analysis results

Building	Performance level	Roof displacement (in.)	Ductility demand ($\delta_{roof}/\delta_{yield}$)	Base shear force V (kip)	Spectral acceleration ($S_a^{analysis} = Vg/W$)
Three-story	Operational	$\delta_{yield} = 1.727$	1.00	384.50	$0.1184g$
	Immediate occupancy	$\delta_{IO} = 3.276$	1.89	709.07	$0.2183g$
	Life safety	$\delta_{LS} = 11.700$	6.77	1133.35	$0.3489g$
	Collapse prevention	$\delta_{CP} = 23.400$	13.55	1197.40	$0.3687g$
	Complete collapse	$\delta_{collapse} = \infty$	∞	1200.28	$0.3695g$
Nine-story	Operational	$\delta_{yield} = 6.475$	1.00	746.55	$0.0751g$
	Immediate occupancy	$\delta_{IO} = 10.248$	1.58	1116.09	$0.1124g$
	Life safety	$\delta_{LS} = 36.600$	5.65	1441.77	$0.1452g$
	Collapse prevention	$\delta_{CP} = 73.200$	11.31	1458.55	$0.1469g$
	Complete collapse	$\delta_{collapse} = \infty$	∞	1469.27	$0.1479g$

ponent $k = 2$ to form the parabolic load distributions shown in Figs. 5 and 6. The total lateral load increment $\Delta F = \Sigma \Delta F_x$ applied for each iteration of the push-over analysis is equal to the initial base shear force V.

The results of the push-over analyses for the two frames are summarized in Tables 2 and 3 and illustrated in Figs. 7–9. Roof lateral displacements at the various performance levels are given in the third column of Table 2, where displacement δ_{yield} reached at the operational level corresponds to the onset of initial yielding of the frame, displacements δ_{IO}, δ_{LS} and δ_{CP} reached at the

Table 3
Extent of plastic behavior

Building	Performance level	Number of sections (n% plasticity)	
		$n < 100\%$	$n = 100\%$
Three-story	Immediate occupancy	3	2
	Life safety	15	15
	Collapse prevention	3	27
Nine-story	Immediate occupancy	33	1
	Life safety	48	48
	Collapse prevention	30	67

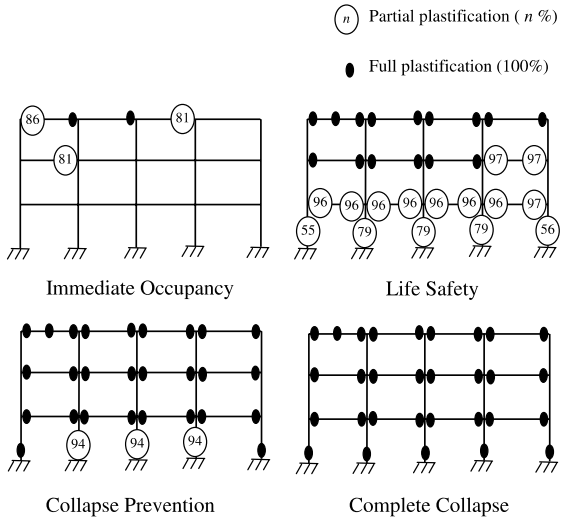

Fig. 7. Performance-level plastic behavior of three-story frame.

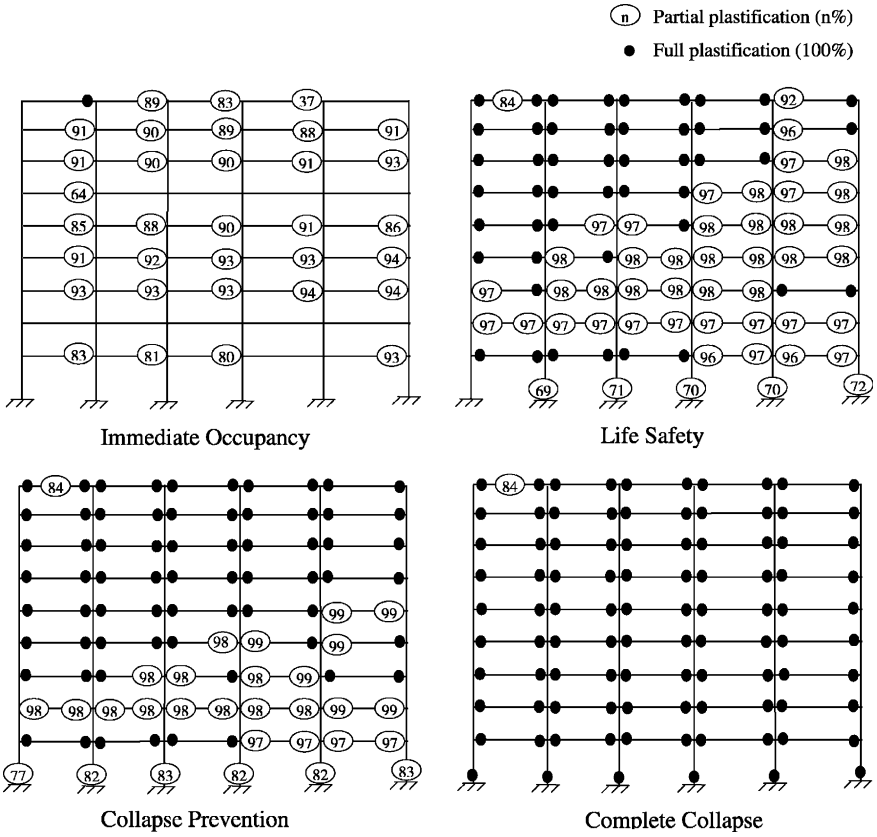

Fig. 8. Performance-level plastic behavior of nine-story frame.

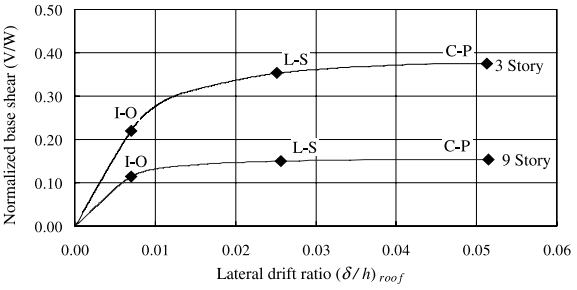

Fig. 9. Push-over curves.

immediate-occupancy, life-safety and collapse-prevention levels are target values equal to 0.7%, 2.5% and 5% of the frame height, respectively [6], and $\delta_{\text{collapse}} = \infty$ signifies the frame has reached the loading level at which it fails in a plastic mechanism mode. The overall ductility demands imposed on the frames at the various performance levels are found through Eq. (12a) and given in the fourth column of Table 2, where $\delta_{\text{roof}} = \delta_{\text{yield}}, \delta_{\text{IO}}, \delta_{\text{LS}}$ or δ_{CP} depending on the performance level, and ductility demand $= \infty$ at the complete-collapse level signifies failure of the frame. (Interstory ductility demands calculated through Eq. (12b) are not presented here in the interest of brevity). The fifth column of Table 2 lists the total base shear forces V (i.e., total lateral inertia loads F) acting on the two frames at the various performance levels (note for both frames that the magnitude of the base shear force at the collapse-prevention level is only slightly less than that at which complete collapse occurs). The spectral accelerations S_a^{analysis} listed in the sixth column of Table 2 for the various performance levels are found through Eq. (10) for base shear forces V from column five of Table 2 and frame total weight $W = \sum w_x$ from column three of Table 1.

Figs. 7 and 8 illustrate the progressive occurrence and extent of plastic behavior at the various performance levels for the frames, where the degrees of plastification indicated for the member sections are found through Eq. (8) for the prevailing values of the plasticity-factor for partially $(1 > p > 0)$ and fully $(p = 0)$ plastic sections, respectively. Plastic yielding occurs at base-support sections of first-story column members and at both end-sections of beam members, which signifies strong-column and weak-beam behavior typical of earthquake-resistant building construction. It is of interest to note

that plastic yielding also occurs at mid-span of the left-most roof beam for both frames. The plastic behavior results are further summarized in Table 3. The normalized push-over curves illustrated for the two frames in Fig. 9 are derived from the results listed in columns three and five of Table 2, where h_{roof} = frame total height (see Figs. 5 and 6).

6. Concluding remarks

The paper has presented a simple computer-based method for push-over analysis of steel building frameworks subject to equivalent-static earthquake loading. The method accounts for first-order elastic and second-order geometric stiffness properties, and the influence that combined stresses have on plastic behavior, and employs a conventional elastic analysis procedure modified by a 'plasticity-factor' to trace elastic–plastic behavior over the range of performance levels for a structure. The plasticity-factor is shown analogous to a similar rigidity-factor for elastic analysis of semi-rigid frames, and the stiffness properties for semi-rigid analysis are directly adopted for push-over analysis. While illustrated for planar frames, the concepts are readily extended to three-dimensional frames by expanding the stiffness matrices given in Appendix A from 6 to 12 degrees-of-freedom and expressing the stiffness elements in terms of in-plane and out-of-plane plasticity-factors [13], and by adopting three-dimensional yield criteria to govern plastic behavior of members under combined stress states involving axial force, biaxial moments and/or torsional moment [8].

Two worked examples illustrate that push-over analysis provides valuable information for the performance-based seismic rehabilitation of existing steel moment-frame buildings. Among other results, the overall ductility demands found through Eq. (12a) provide a basis for checking compliance with global ductility limits, the interstory ductility demands found through Eq. (12b) serve to identify the existence of 'soft' stories, while the S_a^{analysis} values in Table 2 provide a means to assess the adequacy of the earthquake-resistant capacity of a building for corresponding seismic events. The proposed push-over analysis procedure is also an effective tool for the performance-based seismic design of new steel moment-frame buildings; [7].

Acknowledgements

The writers acknowledge the support of the National Science and Engineering Research Council (NSERC) of Canada for research funding and the Post-doctoral Fellowship of the first author. The electronic version of the paper was facilitated by Yanglin Gong, research assistant, University of Waterloo.

Appendix A

For first-order behavior, the stiffness matrix for a member with semi-rigid moment-connections at its ends can be represented as [15]

$$\boldsymbol{K} = \boldsymbol{S}_e \boldsymbol{C}_e \tag{A.1}$$

or, for first- and second-order behavior, as [20]

$$\boldsymbol{K} = \boldsymbol{S}_e \boldsymbol{C}_e + \boldsymbol{S}_g \boldsymbol{C}_g \tag{A.2}$$

where $\boldsymbol{S}_e$ and $\boldsymbol{S}_g$ are respectively the standard first-order elastic and second-order geometric stiffness matrices when the member has 'rigid' moment-connections, and $\boldsymbol{C}_e$ and $\boldsymbol{C}_g$ are corresponding correction matrices that account for the reduced rotational stiffnesses of the 'semi-rigid' moment-connections.

Matrices $\boldsymbol{C}_e$ and $\boldsymbol{C}_g$ are illustrated in the following for the planar beam-column member in Fig. 10, where E is Young's modulus, A and I are respectively the area and moment of inertia of the member cross-section, L is the member length, and R_1 and R_2 are the semi-rigid rotational stiffnesses at the two ends of the member. A, so-called, flexural rigidity-factor r at each end i of the member is defined as [15]

$$r_i = \frac{\alpha_i}{\theta_i} = \frac{1}{1 + (3EI/R_i L)} \quad (i = 1, 2) \tag{A.3}$$

where α_i is the member rotation and θ_i is the total rotation of the connection and the member.

The first-order correction matrix is

$$\boldsymbol{C}_e = \frac{1}{(4 - r_1 r_2)} \begin{bmatrix} e_{11} & 0 & 0 & 0 & 0 & 0 \\ 0 & e_{22} & e_{23} & 0 & 0 & 0 \\ 0 & e_{32} & e_{33} & 0 & 0 & 0 \\ 0 & 0 & 0 & e_{44} & 0 & 0 \\ 0 & 0 & 0 & 0 & e_{55} & e_{56} \\ 0 & 0 & 0 & 0 & e_{65} & e_{66} \end{bmatrix}$$

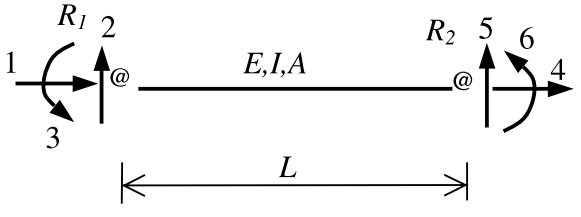

Fig. 10. Planar beam-column member.

where,

$$e_{11} = e_{44} = 4 - r_1 r_2, \quad e_{22} = 4r_2 - 2r_1 + r_1 r_2$$
$$e_{23} = -2Lr_1(1 - r_2), \quad e_{33} = 3r_1(2 - r_2)$$
$$e_{32} = e_{65} = \frac{6}{L}(r_1 - r_2), \quad e_{55} = 4r_1 - 2r_2 + r_1 r_2$$
$$e_{56} = 2Lr_2(1 - r_1), \quad e_{66} = 3r_2(2 - r_1)$$

Having $\boldsymbol{C}_e$ and knowing $\boldsymbol{S}_e$ (see, e.g., [16]), from Eq. (A.1) the first-order elastic stiffness matrix for the member with semi-rigid moment-connections is

$$\boldsymbol{K} = \boldsymbol{S}_e \boldsymbol{C}_e = \frac{1}{(4 - r_1 r_2)} \begin{bmatrix} K_{11} & 0 & 0 & K_{14} & 0 & 0 \\ & K_{22} & K_{23} & 0 & K_{25} & K_{26} \\ & & K_{33} & 0 & K_{35} & K_{36} \\ & \text{SYM} & & K_{44} & 0 & 0 \\ & & & & K_{55} & K_{56} \\ & & & & & K_{66} \end{bmatrix}$$

where,

$$K_{11} = -K_{14} = -K_{41} = K_{44} = \frac{EA(4 - r_1 r_2)}{L}$$
$$K_{22} = -K_{25} = -K_{52} = K_{55} = \frac{12EI(r_1 + r_2 + r_1 r_2)}{L^3}$$
$$K_{23} = K_{32} = -K_{35} = -K_{53} = \frac{6EIr_1(2 + r_2)}{L^2}$$
$$K_{26} = K_{62} = -K_{56} = -K_{65} = \frac{6EIr_2(2 + r_1)}{L^2}$$
$$K_{33} = \frac{12EIr_1}{L}, \quad K_{36} = K_{63} = \frac{6EIr_1 r_2}{L}, \quad K_{66} = \frac{12EIr_2}{L}$$

The second-order correction matrix is

$$\boldsymbol{C}_g = \frac{1}{5(4 - r_1 r_2)^2} \begin{bmatrix} 0 & 0 & 0 & 0 & 0 & 0 \\ 0 & 1 & 0 & 0 & 0 & 0 \\ 0 & g_{32} & g_{33} & 0 & g_{35} & g_{36} \\ 0 & 0 & 0 & 0 & 0 & 0 \\ 0 & 0 & 0 & 0 & 1 & 0 \\ 0 & g_{62} & g_{63} & 0 & g_{65} & g_{66} \end{bmatrix}$$

where,

$$g_{32} = -g_{35} = \frac{-4}{L}\left(8r_1^2 r_2 - 13r_1 r_2^2 - 32r_1^2 - 8r_2^2 + 25r_1 r_2 + 20\right)$$
$$g_{33} = r_1\left(16r_2^2 + 25r_1 r_2^2 - 96r_1 r_2 + 128r_1 - 28r_2\right)$$
$$g_{36} = 4r_2\left(16r_1^2 - 5r_1^2 r_2 + 9r_1 r_2 - 28r_1 + 8r_2\right)$$
$$g_{62} = -g_{65} = \frac{-4}{L}\left(8r_1 r_2^2 - 13r_1^2 r_2 - 32r_2^2 - 8r_1^2 + 25r_1 r_2 + 20\right)$$
$$g_{63} = 4r_1\left(16r_2^2 - 5r_1 r_2^2 + 9r_1 r_2 + 8r_1 - 28r_2\right)$$
$$g_{66} = r_2\left(16r_1^2 + 25r_1^2 r_2 - 96r_1 r_2 - 28r_1 + 128r_2\right)$$

Having $\boldsymbol{C}_g$ and knowing $\boldsymbol{S}_g$ (see, e.g., [16]), from Eq. (A.2) the second-order geometric stiffness matrix for the member with semi-rigid moment-connections is

$$\boldsymbol{S}_g \boldsymbol{C}_g = \frac{N}{5(4 - r_1 r_2)^2} \begin{bmatrix} 0 & 0 & 0 & 0 & 0 & 0 \\ & G_{22} & G_{23} & 0 & G_{25} & G_{26} \\ & & G_{33} & 0 & G_{35} & G_{36} \\ & & & 0 & 0 & 0 \\ & \text{SYM} & & & G_{55} & G_{56} \\ & & & & & G_{66} \end{bmatrix}$$

where N = member axial force and,

$$G_{22} = \frac{2}{L}\left(3r_1^2 r_2^2 + r_1^2 r_2 + r_1 r_2^2 + 8r_1^2 + 8r_2^2 - 34r_1 r_2 + 40\right)$$
$$G_{23} = \frac{1}{2}\left(r_1^2 r_2^2 - 12r_1^2 r_2 + 16r_1 r_2^2 - 28r_1 r_2 + 32r_1^2\right)$$
$$G_{33} = 2L\left(2r_1^2 r_2^2 - 7r_1^2 r_2 + 8r_1^2\right)$$
$$G_{36} = \frac{-L}{2}\left(7r_1^2 r_2^2 - 16r_1^2 r_2 - 16r_1 r_2^2 + 28r_1 r_2\right)$$
$$G_{22} = \frac{1}{2}\left(r_1^2 r_2^2 - 12r_1 r_2^2 + 16r_1^2 r_2 - 28r_1 r_2 + 32r_2^2\right)$$
$$G_{66} = 2L\left(2r_1^2 r_2^2 - 7r_1 r_2^2 + 8r_2^2\right)$$
$$G_{55} = -G_{25} = G_{22}; \quad G_{35} = -G_{23}; \quad G_{56} = -G_{26}$$

Note: The rigidity-factors r in the foregoing matrices for semi-rigid analysis are interchangeable with plasticity-factors p for push-over analysis.

References

[1] AISC. Manual of Steel Construction, Load and Resistance Factor Design. American Institute of Steel Construction, Chicago, IL, 1994.

[2] Biggs JM. Introduction to structural dynamics. USA: McGraw-Hill; 1964.

[3] Cohn MZ. Analysis and design of inelastic structures-volume 2: problems. Ontario, Canada: University of Waterloo Press; 1972.

[4] Chopra AK. Dynamics of structures—theory and applications to earthquake engineering. New Jersey: Prentice-Hall; 1995.

[5] Faella G, Kilar V. Asymmetric multistory R/C frame structures: push-over versus nonlinear dynamic analysis. In: Proceedings of 11th European Conference on Earthquake Engineering. Rotterdam: Balkema; 1998. p. 1–10.

[6] Federal Emergency Management Agency. NEHRP guidelines for the seismic rehabilitation of buildings, Rep. FEMA 273 (Guidelines) and 274 (Commentary), Washinton, DC, 1997.

[7] Gong Y. Optimal performance-based design of building frameworks under seismic loading, PhD Thesis. University of Waterloo, Ontario, Canada, 2002, in preparation.

[8] Grierson DE, Abdel-Baset SB. Plastic analysis under combined stresses. J Engng Mech Div, ASCE 1977;103(5): 837–54.

[9] Gupta A, Krawinkler H. Seismic demands for performance evaluation of steel moment resisting frame structures. John

A. Blume Earthquake Engng. Ctr. Rep. No. 132, Dept. of Civil Engineering, Stanford University, Stanford, California, 1999.

[10] Gupta A, Krawinkler H. Behavior of ductile SMRFs at various seismic hazard levels. J Struct Engng, ASCE 2000;126(1):98–107.

[11] Kilar V, Fazfar P. Simple push-over analysis for asymmetric buildings. Earthquake Engng Struct Dyn 1997;26: 233–49.

[12] Lawson RS, Vance V, Krawinkler H. Nonlinear static push-over—Analysis, why when and how? In: Proceedings of the 5th US National Conference on Earthquake Engineering, vol. 1. Chicago, Illinois: EERI; 1994. p. 283–92.

[13] Liu Y. Optimal design of buildings against progressive collapse under abnormal loading, PhD Thesis. University of Waterloo, Ontario, Canada, 2002, in preparation.

[14] Moghadam AS, Tso WK. 3-D push-over analysis for eccentric buildings. In: Proceedings of the 11th European Conference on Earthquake Engineering, Montreal, 1995. p. 285–92.

[15] Monfortoon GR, Wu TS. Matrix analysis of semi-rigidly connected steel frames. J Struct Div, ASCE 1963;89(6):13–42.

[16] Przemieniecki JS. In: Theory of matrix structural analysis. New York: McGraw-Hill; 1968. p. 81,391.

[17] Saidi M, Sozen MA. Simple nonlinear seismic analysis of R/C structures. J Struct Div, ASCE 1981;107(5):937–52.

[18] UBC. Structural Engineering Design Provisions, Uniform Building Code, vol. 2. International Building Officials, 1994.

[19] Whittaker A, Constantnou M, Tsopelas P. Displacement estimates for performance-based seismic design. J Struct Div, ASCE 1998;124(8):905–12.

[20] Xu L. Geometrical stiffness and sensitivity matrices for optimization of semi-rigid steel frameworks. Struct Optim 1992;5(1–2):95–9.

[21] Xu L, Sherbourne AN, Grierson DE. Optimal cost design of semi-rigid, low-rise industrial frames. Engng J, AISC, 3rd quarter 1995:87–97.